Engineering Structures 33 (2011) 689–695

Contents lists available at ScienceDirect

Engineering Structures

journal homepage: www.elsevier.com/locate/engstruct

Review article

The influence of bending and shear stiffness and rotational inertia in vibrations of cables: An analytical approach

R.A. Sousa [a,c,*], R.M. Souza [b], F.P. Figueiredo [c], I.F.M. Menezes [c]

[a] Pontifical Catholic University of Rio de Janeiro, Civil Engineering Department, Brazil
[b] Department of Civil Engineering, Federal University of Pará, Brazil
[c] Tecgraf/PUC-Rio, Computer Graphics Technology Group, Brazil

ARTICLE INFO

Article history:
Received 13 July 2010
Received in revised form
18 October 2010
Accepted 15 November 2010
Available online 17 December 2010

Keywords:
Vibration of cables
Dynamical analysis
Transmission line conductors

ABSTRACT

The main objective of this work is to analyze the influence of bending and shear stiffness, and rotational inertia in the natural frequencies of overhead transmission line conductors, and to compare the results with a vibrating string, where only geometrical stiffness is considered. Five formulations, based on Bernoulli's and Timoshenko's beam theories, taking into account the effects of geometrical, bending and shear stiffness and rotational inertia are considered here. They are also based on the assumption that the cable is inextensible. The equation of motion of the vibrating cable is developed analytically, assuming small strains. The Newton–Raphson method is employed for the solution of the nonlinear equations. A numerical example is presented and the results are compared with solutions obtained from the technical literature.

Contents

1. Introduction

A very important application in the area of cable vibration that results in many studies and publications is the vibrating behavior of overhead transmission line conductors. A historical review of the string vibration problem was presented by Bassalo [1]. He emphasizes that during the years of 1732 and 1733 Daniel Bernoulli, John Bernoulli's son, studied small vibrations of a string of negligible weight, suspended in both ends and loaded with many equally spaced masses. Bassalo pointed out that Daniel had also worked with non-uniformly thick strings. According to Bassalo [1], D'Alembert in 1746 had studied the string vibration problem. He discussed the problem of a vibrating tensioned string, in which he arrived at a partial differential equation that describes the behavior of a vibrating string. Irvine [2] pointed out that the first study about the shape of a suspended string subjected to its own weight is attributed to Galileo. The main contribution of this work was to present the similarity between this curve and a parabola. In 1691, a group of geographers and mathematicians obtained the analytical solution of this curve, which was called catenary. Ervik et al. [3] presented a review of the most important theoretical aspects of aeolic vibration, such as wind energy, conductor dumping, vibration level, tension, and turbulence effects on cables. They also presented studies about the stochastic properties of wind and its origin and behavior. Another very important aspect of this work was the derivation of analytical expressions for the calculation of conductor vibration levels. Abramovich and Elishakoff [4], following Timoshenko's suggestion, omitted the term representing the joint action of rotational inertia and shear deformation from the differential equations of motion. Abramovich and Elishakoff [5] commented that the classical Bernoulli–Euler theory of flexural behavior of an elastic beam has been known to be inadequate for vibration of higher modes and showed numerical examples

* Corresponding author at: Pontifical Catholic University of Rio de Janeiro, Civil Engineering Department, Brazil. Tel.: +55 21 3527 2113; fax: +55 21 3527 2500.
E-mail address: rflsousa@tecgraf.puc-rio.br (R.A. Sousa).

0141-0296/$ – see front matter © 2010 Elsevier Ltd. All rights reserved.
doi:10.1016/j.engstruct.2010.11.026

for ten different boundary conditions. In this work the authors pointed out that Bresse and Lord Rayleigh introduced the effect of rotational movements of the beam elements in addition to the transverse ones. Abramovich and Hamburger [6] investigated the influence of rotational inertia and shear deformation on the natural frequencies of a cantilever beam with a tip mass. They showed that a vibrating cantilever having a tip mass can serve as a basic model for several structures such as a mast antenna, towers or a flexible robot arm. Maurizi and Bellés [7] studied the natural frequencies of the beam–mass system of a simply uniform beam using the Timoshenko's theory. Rossi et al. [8] presented the free vibration of Timoshenko's beam carrying elastically mounted, concentrated masses. Diana et al. [9] studied an analytical approximation for the definition of the dynamic behavior of cables in turbulent conditions due to vortices. The simulation was performed by means of the finite element method, and the vortex effects were reproduced by nonlinear equivalent oscillations. Posiadala [10] examined the free vibrations of uniform Timoshenko's beam with attachments by means of the Lagrange multiplier approach. Wu and Chen [11] investigated free vibration analysis of a multistep Timoshenko beam carrying lumped masses with eccentricity and rotational inertias. They also presented [12] the exact solution of a single-span uniform Timoshenko's beam carrying any number of spring–mass systems by using numerical assembly method. Aranha Júnior and Souza [13] proposed a finite beam element to analyze static and dynamic behavior taking into account the geometrical nonlinearity. They showed how to consider distributed loads using a co-rotational formulation. This element was used to simulate the behavior of overhead transmission line cables. Lin and Tsai [14] extended the theory of the numerical assembly method to investigate the free vibration characteristic of a multispan Timoshenko's beam carrying multiple point masses, linear and rotational springs and taking into account the rotational inertia. Do and Pan [15] in their studies about transverse motion of marine risers with dynamic actuators, commented that Bernoulli's theory is satisfactory for modeling low-frequency vibrations of beams. Lin [16] included rotational inertias, point masses, linear springs, rotational springs and spring–mass systems to determine the exact natural frequencies and vibration modes of the Timoshenko's beam carrying a number of concentrated elements using the numerical assembly method.

This paper is organized as follows. Section 2 explains how the vertical displacements are obtained according to Bernoulli's theory. Section 3 describes how to obtain the vertical displacements and rotations according to Timoshenko's theory. Section 4 presents a detailed explanation of the ideas proposed herein by means of a numerical example. Finally, Section 5 presents the conclusions about this work.

2. Bernoulli's beam theory

Bernoulli's beam theory is based on the assumption that the cross sections of the beam remain flat and perpendicular to the reference axis, after deformation occurs. Therefore, it is possible to write:

$$\tan[\theta(x,t)] \cong \theta(x,t) = \frac{\partial v(x,t)}{\partial x} \tag{1}$$

where "$\theta(x,t)$" represents the rotation of a generic cross section and "$v(x,t)$" is the vertical displacements. A general formulation, using Bernoulli's beam theory, for the determination of natural frequencies of cables must take into account geometrical and bending stiffness as well as the rotational inertia.

Two formulations are presented based on Bernoulli's beam theory. The first one considers the effects of geometrical and bending stiffness, and the second formulation considers the effects of geometrical and bending stiffness as well as rotational inertia.

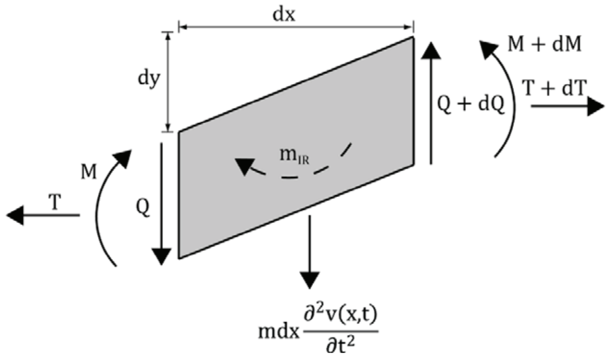

Fig. 1. Infinitesimal element considering rotational inertia.

Fig. 1 shows the free body diagram of an infinitesimal cable element oriented along the x axis at a time-step t.

In Fig. 1, T is the axial force, m is the mass per unit length, $Q(x,t)$ is the shear force, $M(x,t)$ is the bending moment, dx is the infinitesimal element length, dv is the vertical displacement increment and, $m_{IR}(x,t)$ is the rotational inertia, which can be expressed as:

$$m_{IR}(x,t) = \left(\frac{mI}{A}\right)\frac{\partial^2\theta(x,t)}{\partial t^2} \tag{2}$$

where A is the cross section area, I is the moment of inertia and θ is the angle of rotation of the cross section. From the force balance equation in the vertical direction, one can write:

$$\frac{\partial Q(x,t)}{\partial x} = m\frac{\partial^2 v(x,t)}{\partial t^2}. \tag{3}$$

The moment balance equation can be expressed by:

$$\frac{\partial M(x,t)}{\partial x} = -Q(x,t) + T\frac{\partial v(x,t)}{\partial x} + m_{IR}(x,t). \tag{4}$$

The constitutive equation is given by:

$$M(x,t) = EI\frac{d^2 v(x,t)}{dx^2}. \tag{5}$$

Combining the first derivative of Eq. (4), with respect to x, to Eqs. (3) and (5), leads to the following fourth order partial differential equation:

$$EI\frac{\partial^4 v(x,t)}{\partial x^4} - T\frac{\partial^2 v(x,t)}{\partial x^2} + m\frac{\partial^2 v(x,t)}{\partial t^2} - \frac{mI}{A}\frac{\partial^2}{\partial x^2}\left(\frac{\partial^2 v(x,t)}{\partial t^2}\right) = 0. \tag{6}$$

Using the Method of Separation of Variables, such that $v(x,t) = w(x)q(t)$, and assuming a harmonic solution for the function $q(t)$, i.e., $q(t) = \sin(\omega t + \phi)$, where ω is the angular frequency and ϕ is the phase angle, the following expression can be obtained:

$$\sin(\omega t + \phi)\left[w^{\text{iv}}(x) - \frac{T}{EI}w''(x) - \frac{m\omega^2}{EI}w(x) + \frac{m\omega^2}{EA}w''(x)\right] = 0. \tag{7}$$

Avoiding the trivial solution, i.e., "$\sin(\omega t + \phi) = 0$" and using the differential operator ($D = d/dt$), Eq. (7) can be rewritten as:

$$\left[D^4 + 0D^3 + \left(\frac{m\omega^2}{EA} - \frac{T}{EI}\right)D^2 + 0D + \left(-\frac{m\omega^2}{EI}\right)\right]w(x) = 0 \tag{8}$$

or:

$$(D^4 + 0D^3 + BD^2 + 0D + R)w(x) = 0 \quad (9)$$

where:

$$B = \left(\frac{m\omega^2}{EA} - \frac{T}{EI}\right) \quad \text{and} \quad R = \left(-\frac{m\omega^2}{EI}\right). \quad (10)$$

Comparing Eq. (8) with a complete 4th degree polynomial, where the coefficients can be expressed as combinations of its roots, one can obtain:

$$\begin{aligned}(x-a)(x-b)(x-c)(x-d) &= x^4 - (a+b+c+d)x^3 \\ &\quad + (ab+ac+ad+bc+bd+cd)x^2 \\ &\quad - (bcd+acd+abd+abc)x + abcd \\ &= x^4 + Ax^3 + Bx^2 + Cx + R \quad (11)\end{aligned}$$

which leads to the following system of equations:

$$\begin{cases} a+b+c+d = A = 0 \\ ab+ad+ac+bc+bd+cd = B \\ abc+bcd+acd+abd = C = 0 \\ abcd = R. \end{cases} \quad (12)$$

According to Ervik et al. [3], the solution of the above system of equations is:

$$a = +\delta, \qquad b = -\delta, \qquad c = +\mathrm{i}\beta \quad \text{and} \quad d = -\mathrm{i}\beta \quad (13)$$

where

$$\delta = \sqrt{\frac{-B + \sqrt{B^2 - 4R}}{2}} \quad \text{and} \quad \beta = \sqrt{\frac{B + \sqrt{B^2 - 4R}}{2}}. \quad (14)$$

It is important to mention that, according to Eq. (10), δ and β are defined as functions of the frequency (ω). The general solution for this case, considering the contribution of n modes, can be expressed as [3]:

$$\begin{aligned}v(x,t) = \sum_{i=1}^{n} &\sin(\omega_i t + \phi_i)[C_1\cosh(x\delta_i) + C_2\sinh(x\delta_i) \\ &+ C_3\cos(x\beta_i) + C_4\sin(x\beta_i)]. \quad (15)\end{aligned}$$

The boundary conditions considered in this work are the same used by Ervik et al. [3] and are illustrated in Fig. 2, i.e.:

$w(0) = 0$, at $x = 0$;
$w'(0) = 0$, at $x = 0$;
$w(L) = 0$, at $x = L$;
$w''(L) = 0$, at $x = L$.

The imposition of boundary conditions leads to the following relations:

$$C_1 = \frac{C_4\beta}{\delta}\tanh(L\delta), \qquad C_2 = -\frac{C_4\beta}{\delta}, \qquad C_3 = -\frac{C_4\beta}{\delta}\tanh(L\delta) \quad (16)$$

and

$$\tanh(L\delta) = \frac{\delta}{\beta}\tan(L\beta). \quad (17)$$

The natural frequencies of the structure can be obtained by solving the following nonlinear equation "$F_{\mathrm{Bernoulli}}(\omega) = 0$", where:

$$F_{\mathrm{Bernoulli}}(\omega) = \tanh(L\delta(\omega)) - \frac{\delta(\omega)}{\beta(\omega)}\tan(L\beta(\omega)). \quad (18)$$

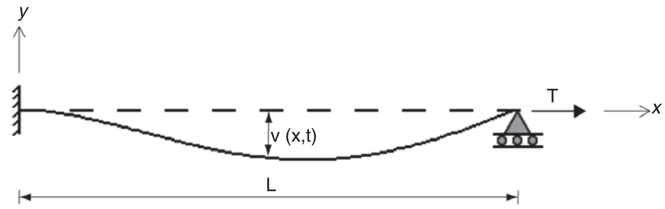

Fig. 2. Boundary conditions.

Finally, the solution for the displacements of the beam according to Bernoulli's theory and considering the contribution of n modes is given by:

$$\begin{aligned}v(x,t) = \sum_{i=1}^{n} C_4 \sin(\omega_i t + \phi_i)\Big\{&\sin(x\beta_i) - \frac{\beta_i}{\delta_i}[\sinh(x\delta_i) \\ &+ \tanh(L\delta_i)[\cos(x\beta_i) - \cosh(x\delta_i)]]\Big\}. \quad (19)\end{aligned}$$

The solution for the second formulation is obtained following the same steps presented above for the first formulation. The only differences are in the values of the coefficients B and R (see Eq. (10)).

3. Timoshenko's beam theory

Timoshenko's beam theory is based on the assumption that the cross sections of a beam remain flat but not necessarily perpendicular to the reference axis, after deformations occur.

In this section, two formulations based on Timoshenko's beam theory are presented. The first one considers the effects of geometrical, shear, and bending stiffness. The second formulation, which is the most complete formulation presented herein, considers geometrical, bending, and shear stiffness as well as rotational inertia effects.

Here, the equilibrium equations are exactly the same as those used by Bernoulli's beam theory (see Eqs. (3) and (4)), except for the constitutive relations, which for this case is given by:

$$M(x,t) = EI\varphi(x,t) = EI\frac{\partial\theta(x,t)}{\partial x} \quad \text{and} \quad Q(x,t) = GA\gamma_{xy}(x,t) \quad (20)$$

where E is the longitudinal elasticity modulus, G is the transversal elasticity modulus, $\varphi(x,t)$ is the curvature, and

$$\gamma_{xy}(x,t) = \frac{\partial v(x,t)}{\partial x} - \theta(x,t) \quad (21)$$

is the shear distortion. Combining Eqs. (3), (4), (20) and (21) one can obtain:

$$GA\frac{\partial^2 v(x,t)}{\partial x^2} - GA\frac{\partial\theta(x,t)}{\partial x} - m\frac{\partial^2 v(x,t)}{\partial t^2} = 0 \quad (22)$$

$$EI\frac{\partial^2\theta(x,t)}{\partial x^2} + GA\frac{\partial v(x,t)}{\partial x} - GA\theta(x,t) - T\frac{\partial v(x,t)}{\partial x} - \frac{mI}{A}\frac{\partial^2\theta(x,t)}{\partial t^2} = 0. \quad (23)$$

Isolating $\partial\theta(x,t)/\partial x$ term from Eq. (22) leads to:

$$\theta'(x,t) = v''(x,t) - \frac{m}{GA}\ddot{v}(x,t). \quad (24)$$

The second derivative of Eq. (24), with respect to x, gives:

$$\theta'''(x,t) = v^{\mathrm{iv}}(x,t) - \frac{m}{GA}\frac{\partial^2\ddot{v}(x,t)}{\partial x^2} \quad (25)$$

and the second derivative of Eq. (24), with respect to t, gives:

$$\frac{\partial^2\theta'(x,t)}{\partial t^2} = \frac{\partial\ddot{\theta}(x,t)}{\partial x} = \frac{\partial^2 v''(x,t)}{\partial t^2} - \frac{m}{GA}\frac{\partial^4 v(x,t)}{\partial t^4}. \tag{26}$$

The derivative of Eq. (23), with respect to x, is given by:

$$EI\theta'''(x,t) + GAv''(x,t) - GA\theta'(x,t) - Tv''(x,t) - \frac{mI}{A}\frac{\partial\ddot{\theta}(x,t)}{\partial x} = 0. \tag{27}$$

Substituting Eqs. (24)–(26) into Eq. (27) leads to:

$$EIv^{\text{iv}}(x,t) - \frac{mEI}{GA}\frac{\partial^2\ddot{v}(x,t)}{\partial x^2} + m\ddot{v}(x,t) - Tv''(x,t) - \frac{mI}{A}\frac{\partial^2 v''(x,t)}{\partial t^2} + \frac{m^2}{GA^2}\frac{\partial^4 v(x,t)}{\partial t^4} = 0 \tag{28}$$

where the only unknown is $v(x,t)$. Using the Method of Separation of Variables, such that $v(x,t) = w(x)q(t)$ gives:

$$EI\sin(\omega t+\phi)w^{\text{iv}}(x) + \frac{mEI\omega^2\sin(\omega t+\phi)w''(x)}{GA} - m\omega^2\sin(\omega t+\phi)w(x) - T\sin(\omega t+\phi)w''(x) + \frac{mI\omega^2\sin(\omega t+\phi)w''(x)}{A} + \frac{m^2I\omega^4\sin(\omega t+\phi)w(x)}{GA^2} = 0. \tag{29}$$

Avoiding the trivial solution, i.e., "$\sin(\omega t+\phi) = 0$", Eq. (29) can be rewritten as:

$$w^{\text{iv}}(x) + \left(\frac{m\omega^2}{GA} + \frac{m\omega^2}{EA} - \frac{T}{EI}\right)w''(x) + \left(\frac{m^2\omega^4}{EGA^2} - \frac{m\omega^2}{EI}\right)w(x) = 0. \tag{30}$$

Using the differential operator ($D = \mathrm{d}/\mathrm{d}t$), Eq. (30) can be expressed as:

$$\left[D^4 + 0D^3 + \left(\frac{m\omega^2}{GA} + \frac{m\omega^2}{EA} - \frac{T}{EI}\right)D^2 + 0D + \left(\frac{m^2\omega^4}{EGA^2} - \frac{m\omega^2}{EI}\right)\right]w(x) = 0 \tag{31}$$

or:

$$(D^4 + 0D^3 + BD^2 + 0D + R)w(x) = 0 \tag{32}$$

where:

$$B = \left(\frac{m\omega^2}{GA} + \frac{m\omega^2}{EA} - \frac{T}{EI}\right) \quad \text{and} \quad R = \left(\frac{m^2\omega^4}{EGA^2} - \frac{m\omega^2}{EI}\right). \tag{33}$$

Note that Eqs. (9) and (32) are identical for both theories, varying only the values of B and R, which are obtained by Eq. (10) for Bernoulli's beam theory and by Eq. (33) for Timoshenko's beam theory. Thus, the general solution of Eq. (31), considering the contribution of n modes, is given by:

$$v(x,t) = \sum_{i=1}^{n}\sin(\omega_i t+\phi_i)[C_1\cosh(x\delta_i) + C_2\sinh(x\delta_i) + C_3\cos(x\beta_i) + C_4\sin(x\beta_i)] \tag{34}$$

$$\theta(x,t) = \sum_{i=1}^{n}\sin(\omega_i t+\phi_i)\Bigg\{[\delta_i C_1\sinh(x\delta_i) + \delta_i C_2\cosh(x\delta_i) - \beta_i C_3\sin(x\beta_i) + \beta_i C_4\cos(x\beta_i)] + \frac{m\omega_i^2}{GA}\times\left[\frac{C_1}{\delta_i}\sinh(x\delta_i) + \frac{C_2}{\delta_i}\cosh(x\delta_i) + \frac{C_3}{\beta_i}\sin(x\beta_i) + \frac{C_4}{\beta_i}\cosh(x\beta_i)\right]\Bigg\}. \tag{35}$$

The boundary conditions are illustrated in Fig. 2, i.e.:

$v(0,t) = 0$, at $x = 0$;
$\theta(0,t) = 0$, at $x = 0$;
$v(L,t) = 0$, at $x = L$;
$\theta'(L,t) = 0$, at $x = L$.

The imposition of boundary conditions leads to the following relations:

$$C_1 = \frac{C_4 S\delta}{\beta}\tanh(L\delta), \qquad C_2 = \frac{-C_4 S\delta}{\beta}, \qquad C_3 = \frac{-C_4 S\delta}{\beta}\tanh(L\delta), \tag{36}$$

and

$$\tan(L\beta) = \frac{S\delta}{\beta}\tanh(L\delta) \tag{37}$$

where:

$$S = \frac{GA\beta^2 - m\omega^2}{GA\delta^2 + m\omega^2}. \tag{38}$$

The natural frequencies of the structure can be obtained by solving the following nonlinear equation "$F_{\text{Timoshenko}}(\omega) = 0$", where:

$$F_{\text{Timoshenko}}(\omega) = \frac{\beta(\omega)}{\delta(\omega)S(\omega)}\tan(L\beta(\omega)) - \tanh(L\delta(\omega)). \tag{39}$$

Finally, the solutions for the displacements and rotations of the beam according to Timoshenko's theory are given by:

$$v(x,t) = \sum_{i=1}^{n}C_4\sin(\omega_i t+\phi_i)\left\{\sin(x\beta_i) - \frac{\delta_i S_i}{\beta_i}[\sinh(x\delta_i) + \tanh(L\delta_i)[\cos(x\beta_i) - \cosh(x\delta_i)]]\right\} \tag{40}$$

and

$$\theta(x,t) = \sum_{i=1}^{n}C_4\sin(\omega_i t+\phi_i)\Bigg\{\cos(x\beta_i)\left(\frac{GA\beta_i^2 - m\omega_i^2}{GA\beta_i}\right) - \frac{\delta_i S_i}{\beta_i}\Bigg[\cosh(x\delta_i)\left(\frac{GA\delta_i^2 + m\omega_i^2}{GA\delta_i}\right) - \tanh(L\delta_i)\left[\sin(x\beta_i)\left(\frac{GA\beta_i^2 - m\omega_i^2}{GA\beta_i}\right) + \sinh(x\delta_i)\left(\frac{GA\delta_i^2 + m\omega_i^2}{GA\delta_i}\right)\right]\Bigg]\Bigg\}. \tag{41}$$

4. Numerical example

The natural frequencies have been obtained by means of the implicit transcendental Eqs. (18) and (39) for Bernoulli's and Timoshenko's beam theories, respectively. In order to solve

Table 1
Parameters for Bernoulli's theory.

Bernoulli			
	Bending stiffness	Bending stiffness and rotational inertia	Ervik
B	$B_F = -\frac{T}{EI}$	$B_{FR} = \left(\frac{m\omega^2}{EA} - \frac{T}{EI}\right)$	$B_{\mathrm{ERVIK}} = -\frac{T}{EI}$
R	$R_F = -\frac{m\omega^2}{EI}$	$R_{FR} = -\frac{m\omega^2}{EI}$	$R_{\mathrm{ERVIK}} = -\frac{m\omega^2}{EI}$
S	–	–	–
$F(\omega)$	$F_F(\omega) = \tanh(\delta_F L) - \frac{\delta_F}{\beta_F}\tan(\beta_F L)$	$F_{FR}(\omega) = \tanh(\delta_{FR} L) - \frac{\delta_{FR}}{\beta_{FR}}\tan(\beta_{FR} L)$	$F_{\mathrm{ERVIK}}(\omega) = \sin(\beta_{\mathrm{ERVIK}} L)$

Table 2
Parameters for Timoshenko's theory.

Timoshenko			
	Bending stiffness and shear stiffness	Bending stiffness, shear stiffness and rotational inertia	Geometrical stiffness
B	$B_{FR} = \left(\frac{m\omega^2}{GA} - \frac{T}{EI}\right)$	$B_{FR} = \left(\frac{m\omega^2}{GA} + \frac{m\omega^2}{EA} - \frac{T}{EI}\right)$	–
R	$R_{FS} = -\frac{m\omega^2}{EI}$	$R_{FSR} = \left(\frac{m^2\omega^4}{EGA^2} - \frac{m\omega^2}{EI}\right)$	–
S	$S_{FS} = \frac{GA\beta_{FS}^2 - m\omega^2}{GA\delta_{FS}^2 + m\omega^2}$	$S_{FSR} = \frac{GA\beta_{FSR}^2 - m\omega^2}{GA\delta_{FSR}^2 + m\omega^2}$	–
$F(\omega)$	$F_{FS}(\omega) = \tanh(\delta_{FS} L) - \frac{\beta_{FS}}{\delta_{FS} S_{FS}}\tan(\beta_{FS} L)$	$F_{FSR}(\omega) = \tanh(\delta_{FSR} L) - \frac{\beta_{FSR}}{\delta_{FSR} S_{FSR}}\tan(\beta_{FSR} L)$	$F_G(\omega) = \sin\left(\omega\sqrt{\frac{m}{T}}L\right)$

Table 3
Natural frequencies for all formulations.

Vibration mode	F_F (Hz)	F_{FR} (Hz)	F_{ERVIK} (Hz)	F_{FS} (Hz)	F_{FSR} (Hz)
1	1.35007	1.35007	1.34832	1.35006	1.35006
25	33.92474	33.92464	33.88085	33.92440	33.92430
50	68.8792	68.87837	68.78972	68.87685	68.87602
75	105.84274	105.83987	105.70467	105.83486	105.83199
100	145.70383	145.6968	145.51344	145.68477	145.67776
125	189.23528	189.22102	188.98870	189.19684	189.18261
150	237.08600	237.06027	236.77961	237.01688	236.99123
175	289.78576	289.74297	289.41648	289.67101	289.62837
200	347.75814	347.69107	347.32347	347.57857	347.51177
225	411.33693	411.23654	410.83495	411.06843	410.96852
250	480.78277	480.63793	480.21205	480.39571	480.25167
281	575.34343	575.12449	574.68608	574.75886	574.54137

such equations, the Newton–Raphson method is employed. The natural frequencies of the cables correspond to the roots of these equations. The starting point of the numerical procedure (ω_0) is the lowest natural frequency for the case where only geometrical stiffness is considered (i.e., $\omega_0 = \sqrt{(\pi^2 T)/(L^2 m)}$). The Newton–Raphson method is then used to obtain the next roots of Eqs. (18) and (39).

Tables 1 and 2 show the formulations of Bernoulli's and Timoshenko's beam theories with all necessary parameters for computing natural frequencies according to the corresponding formulations. Table 3 shows, for each vibration mode, the corresponding values of the natural frequencies for the numerical example presented herein.

Since Ervik's formulation [3] is based on Bernoulli's theory, it is placed in Table 1, for comparison purpose. Similarly, for the case of Timoshenko's theory (Table 2) the solution of a vibrating string is placed in the third column.

Except for $F_G(\omega)$ function, which represents an analytical solution, the other functions $F_F(\omega)$, $F_{FR}(\omega)$, $F_{FS}(\omega)$ and $F_{FSR}(\omega)$ were solved numerically by means of the Newton–Raphson method. The obtained results are the roots of each function which represent the natural frequencies of the structures. The numerical input data is related to an aluminum alloy 6061 T6: $T = 20{,}000$ N, $L = 200$ m, $E = 69{,}637{,}055$ kN/m^2, $D = 0.025$ m and $m_a = 2.7145$ kg/m^3. The range of the analyzed frequencies was from 0 to 600 Hz (0–3770 rad/s), which corresponds to vibration modes 1 and 281, respectively.

In order to evaluate the difference in phase between two different formulations as well as the number of "dephased" vibration modes between these two formulations, a new parameter, named Mode Factor, has been defined according to the following expression:

$$\text{Mode Factor} = \frac{\left|F_{X_n} - F_{FSR_n}\right|}{F_{FSR_n} - F_{FSR_{n-1}}} \quad (42)$$

where F_{X_n} is the value of a natural frequency of mode n, for a formulation "X", and F_{FSR_n} and $F_{FSR_{n-1}}$ are the frequencies corresponding to modes n and $n-1$, respectively, for the most precise formulation.

When the *Mode Factor* is larger than one, it means that the two formulations are approximately dephased by one vibration mode; when the factor is equal to two, it indicates a difference in phase of approximately two vibration modes, and so on.

In addition to this parameter, the frequencies obtained with all formulations are also compared to the frequencies obtained with the most precise formulation.

For the sake of simplicity, the results corresponding to the function "$F_G(\omega)$" were omitted, because its error in Fig. 3, w.r.t. to the function "$F_{FSR}(\omega)$" is approximately 35% at the 281st vibration mode and the corresponding *Mode Factor* is approximately equal to 60.

Fig. 3 shows that the parameter $F_{\mathrm{ERVIK}}(\omega)$ decreases from 0.13% at the 1st vibration mode until it reaches zero and increases (in absolute value) again until it reaches approximately 0.023% at the

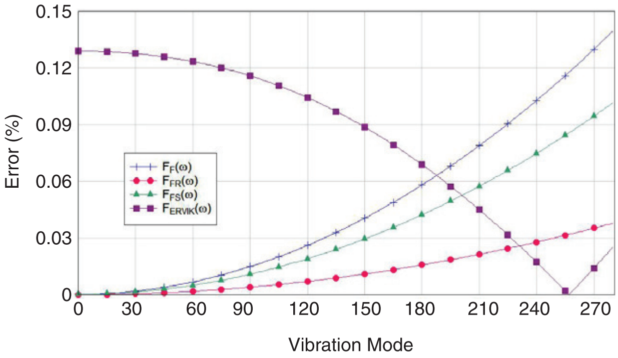

Fig. 3. Error corresponding to functions $F_F(\omega)$, $F_{FR}(\omega)$, $F_{FS}(\omega)$, $F_{\mathrm{ERVIK}}(\omega)$ with respect to function $F_{FSR}(\omega)$.

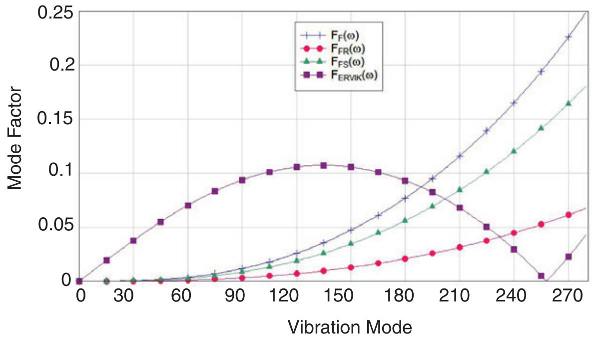

Fig. 4. *Mode Factor* with respect to the vibration mode for functions $F_F(\omega)$, $F_{FR}(\omega)$, $F_{FS}(\omega)$, $F_{\mathrm{ERVIK}}(\omega)$, and $F_{FSR}(\omega)$.

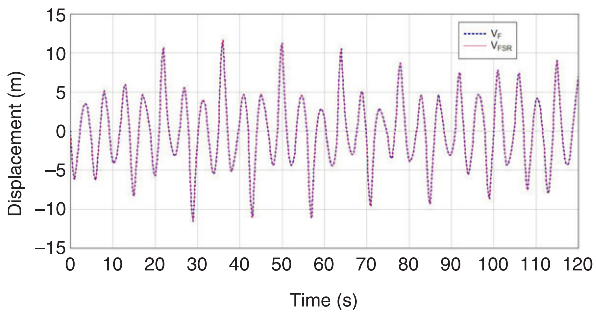

Fig. 5. Vertical displacement time histories for a section located at the center of the cable comparing the case which considers only bending and geometrical stiffness, V_F, with the most general case, V_{FSR}.

281st vibration mode. For the functions $F_F(\omega)$, $F_{FR}(\omega)$ and $F_{FS}(\omega)$ the error increases with the vibration modes.

Fig. 4 shows that the "Mode Factor" corresponding to the function $F_{\mathrm{ERVIK}}(\omega)$ increases up to 0.11% at the 134th vibration mode, then decreases until zero, and then increases again to the value of approximately 0.041 at the 281st vibration mode. The "Mode Factor" of the other formulations always increases with the vibration modes, as shown in the Fig. 4.

Fig. 5 shows the vertical displacement time histories for a section located at the center of the cable. It compares the case where only bending and geometrical stiffness were taken into account, V_F, with the most general case, V_{FSR}, where bending, geometrical and shear stiffness as well as rotational inertia were considered. The initial velocity and displacement used here were 30 km/h and zero, respectively. According to Fig. 5, a maximum relative error of 5% was obtained, during 120 s of analysis.

5. Conclusions

Bernoulli's and Timoshenko's beam theories were used in this paper to determine vibration frequencies of overhead transmission line conductors. In the formulation based on the Timoshenko's theory it is necessary to solve a system of partial differential equations, while in the formulation based on Bernoulli's theory it is only necessary to solve a partial differential equation to determine the vertical displacements and rotations of the cable as a function of time. The equations that allow the determination of the natural frequencies of the cable for any formulation, except the one that considers only geometrical stiffness, are transcendental. In other words, they are implicit trigonometric functions, which do not present analytical solutions, justifying the use of numerical methods.

In the frequency range from 0 to 600 Hz (see Table 3), where there is a predominance of aeolic vibration, the frequency values obtained were in the range of 1.35 Hz, for the first vibration mode, and 574.50 Hz, for the last vibration mode. Furthermore, it can be noticed that the differences among these values, considering each formulation, were very small.

Considering that the most general formulation takes into account all the effects at the beam's cross sections, it was considered to be the most accurate formulation. It was shown that neglecting the effects of bending and shear stiffness and the rotational inertia in the determination of the natural frequencies of the cable can lead to an error of approximately 34%. When the approximation proposed by Ervik et al. [3] is considered, it was noted that the results are very different from the other cases, beginning with an error of 0.12% in the first vibration mode, decreasing until zero in the 263th vibration mode, and increasing to an error of 0.027% in the 281st vibration mode.

It was also observed that the error obtained by neglecting the effects of shear stiffness and/or rotational inertia is very small comparing to the case where bending and geometrical stiffness are considered.

The maximum relative error obtained in the vertical displacement time histories for a section located at the center of the cable was 5%, which demonstrates that the effects of shear stiffness and rotational inertia are negligible when compared with the effects of bending and geometrical stiffness.

Therefore, the comparisons presented in this work lead to the conclusion that the effects of geometrical and bending stiffness must be considered in order to have a more precise determination of the natural frequencies of cables.

Acknowledgement

The authors acknowledge the financial support by Tecgraf (Group of Technology in Computer Graphics), PUC-Rio, Rio de Janeiro, Brazil. The authors also wish to acknowledge Professor José Perilo da Rosa Neto of the Department of Civil Engineering of Federal University of Pará, Brazil, who was always helpful and encouraged the development of this work.

References

[1] Bassalo JMF. Birth of the physics 3500 BC—1900 AC. University Federal of Pará's Publisher; 1996 [in Portuguese].
[2] Irvine HM. Statics of suspended cables. J Struct Div 1975;101:187–205.
[3] Ervik M, Berg A, Boelle A, Claren RF, Dalle B, Edwards AT, et al. Report Aeolian vibration. Electra 1986;124:410–77.
[4] Abramovich H, Elishakoff I. Application of Krein's method for determination of natural frequencies of periodically supported beam based on simplified Bresse–Timoshenko equations. Acta Mech 1987;66:39–59.
[5] Abramovich H, Elishakoff I. Influence of shear deformation and rotary inertia on vibration frequencies via Love's equations. J Sound Vibration 1990;137:516–22.
[6] Abramovich H, Hamburger O. Vibration of a uniform cantilever Timoshenko beam with translational and rotational springs and with a tip mass. J Sound Vibration 1992;154:67–80.

[7] Maurizi MJ, Bellés M. Natural frequencies of the beam–mass system: comparison of the two fundamental theories of beam vibration. J Sound Vibration 1991;150:330–4.
[8] Rossi RE, Laura PAA, Avalos DR, Larrondo H. Free vibrations of Timoshenko beams carrying elastically mounted concentrated masses. J Sound Vibration 1993;165:209–23.
[9] Diana G, Cheli F, Fossati F, Manenti A. Aeolian vibrations of overhead transmission lines computation in turbulence conditions. J Wind Eng Ind Aerodyn 1993;46:639–48.
[10] Posiadala B. Free vibrations of uniform Timoshenko beams with attachments. J Sound Vibration 1997;204:359–69.
[11] Wu JS, Chen CT. A lumped-mass TMM for free vibration analysis of a multi-step Timoshenko beam carrying eccentric lumped masses with rotary inertias. J Sound Vibration 2007;301:878–97.
[12] Wu JS, Chen CT. Free vibration analysis of a Timoshenko beam carrying multiple spring-mass systems by using he numerical assembly technique. Int J Numer Methods Eng 2001;50:1039–58.
[13] Aranha Júnior GYR, Souza RM. Finite Element of frame to nonlinear static and dynamic analyze between of the co-rotational formulation. Jornadas Sud-Americanas de Ingenieria Estructural; 2004 [in Portuguese].
[14] Lin HY, Tsai YC. On the natural frequencies and mode shapes of a multiple-step beam carrying a number of intermediate lumped masses and rotary inertias. Struct Eng Mech 2007;22:701–17.
[15] Do KD, Pan J. Boundary control of transverse motion of marine risers with actuator dynamics. J Sound Vibration 2008;318:768–91.
[16] Lin HY. On the natural frequencies and mode shapes of a multispan Timoshenko beam carrying a number of various concentrated elements. J Sound Vibration 2009;319:593–605.